Transactions of the Royal Society of Edinburgh: Earth Sciences, **97**, 311–324, 2008 (for 2006)

Granitic batholiths: from pervasive and continuous melting in the lower crust to discontinuous and spaced plutonism in the upper crust

Jean Louis Vigneresse

ABSTRACT: The generation of granitic magmas begins with melting in the lower crust, under active participation of the underlying mantle. Thermally driven, melting is a pervasive and continuous process that develops over a wide region. In contrast, the building of a granitic pluton is highly discontinuous in time and space. Several inputs of magma, sometimes with a different chemical compositions, are focused toward a region where they accumulate, forming a large pluton, often separated by some 50 km from an adjacent one. The switch from a continuous to a discontinuous process represents a fundamental point of magma generation. It gives place to the modified model m(M-SAE), in which the mantle (m) and Melting (M) are separated from the Segregation (S), Ascent (A) and Emplacement (E) modes. Discontinuities result from non-linear processes that develop during segregation and ascent of the magma. They rely on the non-linear rheology of partially molten rocks. Thresholds control the change from a solid-like to liquid-like behaviour of the magma. In between, the rheology exhibits sudden jumps between states. Because two phases continuously coexist (matrix and melt), strain is highly partitioned between them. This may induce highly discontinuous melt segregation, which needs both pure and simple shear to develop. Melt focusing is controlled by the viscosity contrast between the two phases. It gives rise to different compaction lengths depending on the region, a partially melting source or a nearly brittle crust, where it develops. Because ascent and emplacement are discontinuous in time, this allows the crust to relax, avoiding the room problem for a pluton intruding the upper crust. Intermediate magma chambers could develop with different temperature and magma composition. They could be the place of enhanced magma mixing. Finally, the stress conditions, which differ for each tectonic setting, influence the shape of the granitic body.

KEY WORDS: ascent, emplacement, granitic pluton, magma mixing, melting, segregation

Granitic intrusions constitute the most effective mode of transporting elements from the lower crust, where melting develops, to the upper crust, where granitic plutons are emplaced. Indeed, granitic magmas actively participate in the evolution and subsequent differentiation of the continental crust. They bring the heat producing elements (Th, U and K) and light minerals into the upper crust. This keeps the continental crust stratified and buoyant, avoiding a large scale recycling into the mantle.

A long-term development since Earth accretion resulted in about 2/3 of the crust being formed at the end of the Archean, at 2·6 Ga (Taylor & McLennan 1995). After that period, crustal formation occurred in sudden bursts, during which huge volumes of pristine crust have been produced, leading to the present continental crust. However, the inspection of individual plutons, as well as studies on the mechanisms that rule granite generation, indicate that the development of one granitic body only requires about 5–10 Ma (Pitcher 1993; Petford *et al.* 2000). This led to the idea that granitic magmas result from a double differentiation effect. The continental crust first differentiates from the mantle. A second process, internal to the crust, leads to crustal differentiation and granite formation (review in Cashman & Bergantz 1991).

A good place for crustal formation is plate margins. The connection of granite generation with active plate margins has long been recognised (Pitcher 1979; Pitcher *et al.* 1985). First, distinction has been made between orogenic and non-orogenic granitoids (Martin & Piwinskii 1972). Those authors considered partial melting of the crust by the ascent of wet peridotite, with the possible influence of a variable amount of aqueous fluid. However, the bulk chemistry of granitic intrusions varies with the degree of continental convergence (Pitcher 1987). Thus, with ongoing collision, the orogenic granites evolve from oceanic arc to the Andinotype, owing to a progressive thickening of the crust, as in the Andes. It is followed by the Hercynotype, corresponding to oblique collision, and ends through the Caledonian-type, with post closure uplift (Pitcher *et al.* 1985). Within that scheme, the granite chemistry, and hence the conditions of formation, evolves from M-type, passing to I-type and to the S-type, depending on the source region (Chappell *et al.* 1987; Chappell & White 2001). It ends with biotite granite, diorite and gabbro (Pitcher 1987). The major assumptions underpinning those concepts of granite formation are the nature of the source region that controls magma composition, and the tectonic settings that control magma ascent. Internal chemical processes as differentiation and/or assimilation modify the magma up to present composition.

Restricting the scale of granite generation to a smaller scale, as observed in a single pluton, indicates a discontinuous mode of magma inputs. Although various chemical and mineralogical facies have long been described within a single pluton, their evolution had been assigned to internal chemical evolution (Hildreth & Moorbath 1988). The popular MASH model (Fig. 1), standing for melting, assimilation, storage and

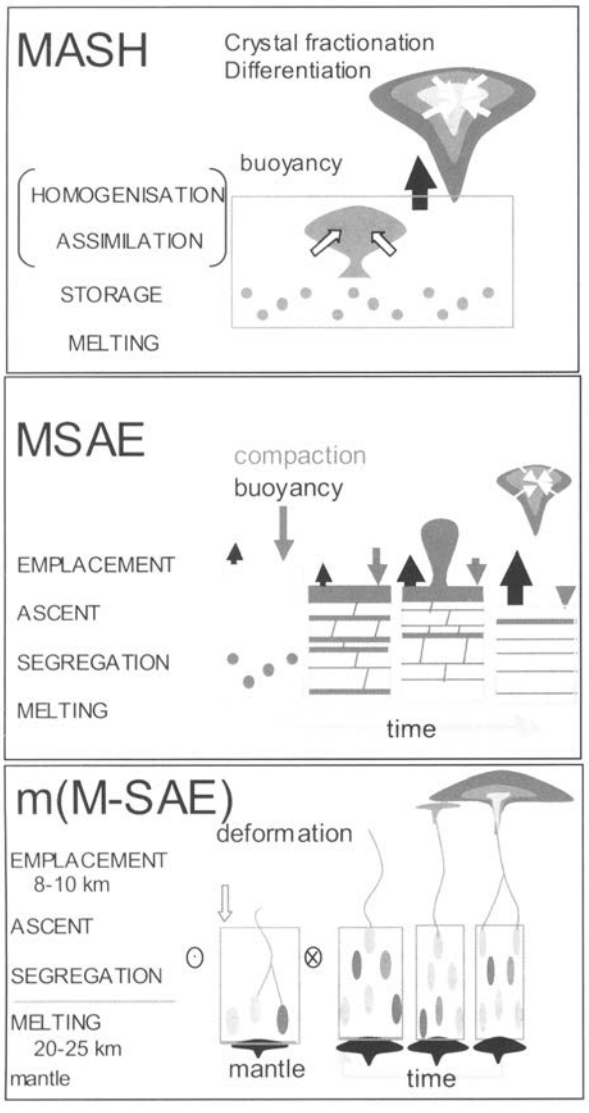

Figure 1 Evolution of the concepts for granite generation, from MASH to MSAE and m(M-SAE). In a first step, the MASH model stands for melting, assimilation, storage and homogenisation (Hildreth & Moorbath 1981). It has been replaced by the MSAE model (Petford *et al.* 1997) with melting segregation, ascent and emplacement. The mantle component has been added and the three last states distinguished from melting, giving place to m(M-SAE).

homogenisation, resulted from field observations. However, the observation of a magmatic fabric within a given facies attesting magma flow (Bouchez 1997) strongly modified our perception of magmatic intrusions. A first step has been to identify four distinct stages that develop during granite generation. These four stages: melting, segregation, ascent and emplacement, gave place to the MSAE model (Petford *et al.* 1997). The stages develop separately, induced by each preceding one and partly controlled by the succeeding one, and they occur on different space and time scales. Melting is ruled by the mineral phases in contact and by the available heat. Segregation is controlled by the amount of melt and the ambient stress field. Ascent is basically stress induced. Emplacement is also ruled by the ambient tectonics stress pattern. Naturally they all depend on the rheological conditions of the crustal material, melt and surrounding rocks. Although these four stages (Vigneresse 2004) had been considered as a succession of four independent processes, melting has been separated from the three late stages and the mantle involvement has been considered, giving place to the m(M-SAE) model (Fig 1), a modified version of the previous MSAE model (Vigneresse 2004). Indeed, the mantle provides material that contributes to modify a specific geochemical composition issued from minerals of the continental crust. It also acts as a heat source for melting and as a stress provider allowing melt segregation. Hence, melt should have been produced in a sufficient quantity to first get connected in the source region and then be able to segregate. The present m(M-SAE) paradigm considers the last three stages as a succession of discontinuous processes that interact cyclically with each other. Segregation starts only after melt has been produced in enough quantity to be able to move, leading to discontinuous magma ascent either through diapirs or dykes. The emplacement of this magma results from successive inputs of magma (Pitcher & Hutton 1982; Glazner *et al.* 2004) sometimes marked by discordant fabric and by age discrepancy between facies.

The switch from a continuous and pervasive melting, mostly controlled by diffusive heat and material from the mantle, to a discontinuous segregation of melt in time and space represents an intriguing problem. It has rarely been addressed in previous studies about granite generation. It came out after long lasting studies devoted to granite generation, but became more obvious after the completion of two independent numerical models of melt segregation (Vigneresse & Burg 2000, 2005; Rabinowicz & Vigneresse 2004). Those two models, as well as analogue experiments (Bauer *et al.* 2000; Rosenberg 2001; Bons *et al.* 2001; Barraud *et al.* 2001; Walte *et al.* 2005) clearly pointed out the discontinuous nature of melt segregation. They also revealed the role played by the specific rheology of partially molten rocks (PMR). Those studies successively identified the controlling parameters as thresholds (Vigneresse *et al.* 1996), strain partitioning (Vigneresse & Tikoff 1999), and instabilities (Burg & Vigneresse 2002). They lead to a more comprehensive model of rheology for PMR (Vigneresse & Burg 2004), specifically designed from field observations.

The present paper is organised from the new paradigm of granite generation, m(M-SAE). It starts by briefly formulating the continuous and pervasive character of melting, driven by the heat coming from the mantle. Then, an introduction to the rheology of PMR reviews the importance of thresholds that separate domains of response of PMR to stress. Strain partitioning and the importance of strain rate impose a full description of PMR rheology. This allows the introduction of the results of numerical modelling through Eulerian description, using analytical expressions (Rabinowicz & Vigneresse 2004), and Lagrangian description, with a cellular automaton (Vigneresse & Burg 2000). Results identify a small window for the input parameters. They show that melt segregation rapidly stops when the amount of melt is outside that window, by lack of melt or loss of cohesion of the matrix. This is also evidenced from field observations. A second point deals with melt focusing, which seems a rarely described mechanism during melt segregation. Discussions and geological consequences of the discontinuities are examined.

1. Pervasive and continuous melting

1.1. Heat source

Partial melting in the lower crustal levels is essentially controlled by heat diffusion and/or advection directly coming out from the mantle or from basaltic intrusions. The role of basalt in generating silicic magmas is also demonstrated by numerous geochemical observations on intermediate and silicic magmas from plutonic complexes. Those felsic magmas are often closely associated with mafic enclaves or dykes attesting a mantle contribution (Furman & Spera 1985; Bacon 1986; Vernon 1990). In some specific cases, for instance alkaline

https://doi.org/10.1017/S0263593300001474 Published online by Cambridge University Press

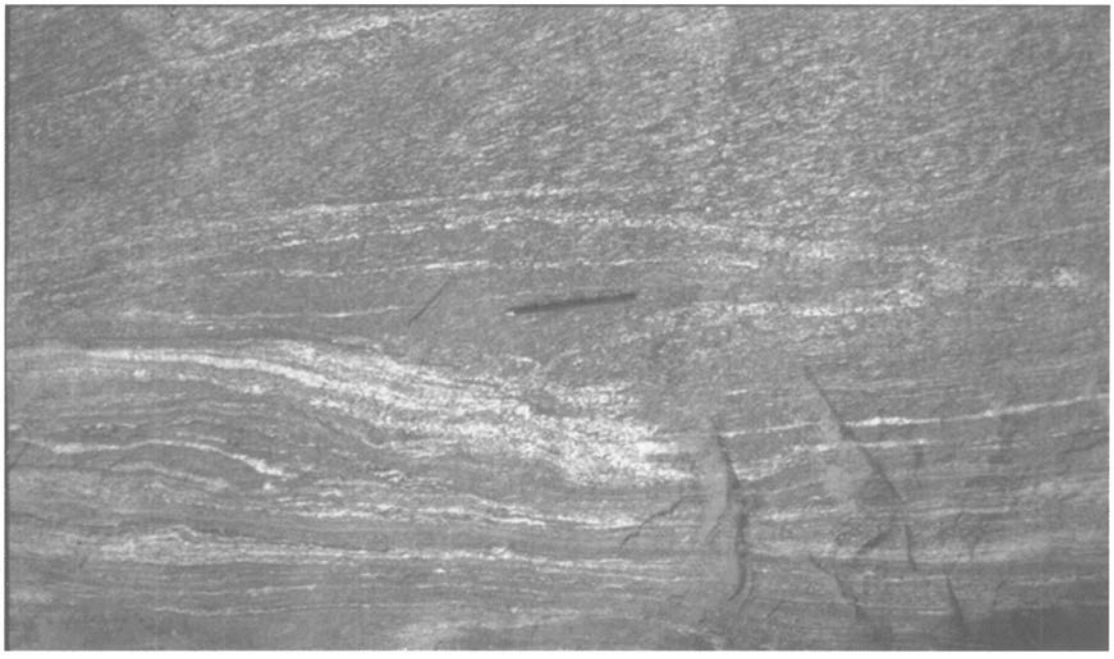

Figure 2 Gneiss from Sierra de Algodão, northeast Brazil undergoing melting. In the upper part of the sample, the amount of melt (8%) is below the threshold for connection, though they are oriented within the foliation plane. Melt motion is unlikely. Conversely, the veins shown on the lower part of the sample document melt motion.

magmas, the mantle component certainly overcomes the crustal one.

Commonly, additional heat, high enough to induce melting, is provided from intrusive material coming from the mantle or by the mantle itself (Thompson 1999). Continuous heating through plate subduction simplifies the problem. When heat results from advection, the amount of melt is limited to about one-sixth of the volume of the intrusive magma (Bergantz 1989). Thus, under-plating basalts to the continental crust results in limited volumes of generated magma. Repeated intrusions of basaltic sills modify the thermal regime of the crust (Petford & Gallagher 2001; Annen & Sparks 2002). Periodic intrusions of basalt at a depth of 20 km create reverse geothermal gradients, the thermal anomalies of which take several million years to decay. However, competition occurs between the heat and fluids required for melting the crust and the heat lost when the intrusion crystallises. After 1·6 Ma of periodic intrusions every 10 ka, and with temperatures of 1100–1300°C, an 8 km-thick basaltic layer develops a temperature anomaly resulting in about 80% of melt production within a fertile crust (Annen & Sparks 2002). The volume, composition and temperature of those melts vary greatly across the intrusion zone. Segregated melts are chemically hybrids with mantle and crustal components. Nevertheless, the very large melt percentage is unrealistic in terms of crustal cohesion. Conversely, a too long periodicity (about 100 ka) is not effective for large-scale melt generation in the crust.

In all other situations, the heat transfer from the mantle to the crust develops through diffusion, which is not a fast process. Hence, biotite dehydration starts above 800°C (Patiño Douce & Beard 1995) whereas the average temperature at the Moho depth ranges from 500°C to 600°C. Assuming a heat diffusivity value of 10^{-6} m/s^2, the characteristic time (τ) for heat transport writes with lengths scaled in km and time in Ma (Crank 1975):

$$\tau = 0{\cdot}03\ L^2 \qquad (1)$$

This means that it takes 30 ka for heat to diffuse along 1 km and 3 Ma when the heat source is located at 10 km from the place of melting. Another possible method of reaching melting temperatures is to double the thickness of the crust, but this takes about 30 Ma (Thompson 1999). In contrast, by thinning the crust, the melting temperature is overcome in the mantle before being reached in the crust, making a thin crust unlikely for producing granitic melts (Thompson 1999).

Whatever the mechanisms required to induce crustal melting, the heating process is slow and also very diffuse in space. The result is that melting is pervasive in the crust, as observed in the field (Fig. 2). In gneisses that underwent partial melting, such as the one shown from the Sierra de Algodão, North Brazil, the melt content is estimated from the leucosome patches. These are about 1–5 cm in length, spaced by about 1 cm along the foliation plane.

1.2. Melting conditions

The role of water during crustal melting is essential. Water commonly lowers the melting point and decreases the viscosity of granitic melts. It also controls melt mobility. Water solubility in granitic melts decreases with shallower depths and with the melt composition. The result is that, depending on the quantity of water a granitic melt can incorporate, it can be segregated and transported upward in the crust. Two types of melting certainly coexist, though not at the same crustal level: water-assisted melting and dehydration melting. In the first case, water must be supplied from external sources, giving place to local melting, as clearly observed in migmatites (Menhert 1968). However, it is unlikely that water occurs as a free phase at depths at which granitic melts are generated.

In the second case, hydrous minerals such as micas or amphiboles liberate OH ions that are immediately reincorporated into granitic melts (Clemens 1990). Melting starts with muscovite dehydration at about 700°C, ending at about 780°C (Harris *et al.* 1995). The reaction produces a volume of melt nearly equivalent to that of the muscovite, provided quartz and plagioclase are in equal quantity and about one third that of the micas (Patiño Douce & Harris 1998). The reaction is enhanced in the presence of water, requiring an amount of plagioclase about double that of the quartz, but it

https://doi.org/10.1017/S0263593300001474 Published online by Cambridge University Press

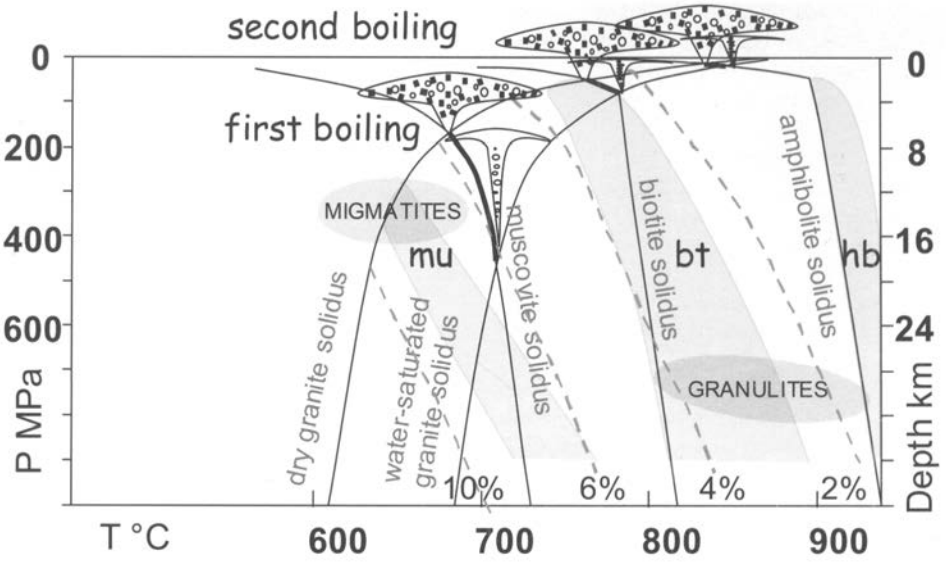

Figure 3 Pressure-temperature diagram showing the solidus curves for muscovite, biotite and amphibole, a proxy for different types of granites. The intersections of those curves with the wet and dry solidus provide the places where first boiling, due to magma decompression, and second boiling, due to crystallisation, occur. The water content in the melt is shown by dashed lines. The fields of muscovite (mu), biotite (bt) and hornblende (hb) are shown in grey. Fields for granulite and migmatites formation are displayed.

results in a volume of melt double to that produced in dry conditions (Patiño Douce & Johnston 1991). Nevertheless, the resulting quantity of melt remains low, owing to the low abundance of muscovite in crustal rocks.

At higher temperatures (780–870°C) biotite starts melting. A quantity of about two thirds quartz and plagioclase, added to one volume of biotite, produces a slightly larger amount of melt with a residual phase that includes K-feldspar and orthopyroxene or garnet. Free water also enhances melt production, whereas pressure shifts the reaction to higher temperature (Patiño Douce & Beard 1995).

At still higher temperatures (above 900°C) hornblende breakdown induces dehydration, leading to melt composition with a reduced K/Na ratio (Whitney 1990). At low pressure, the alkali content of the melt should be derived entirely from hornblende. In contrast, at pressures higher than 2·2 GPa, reactions between hornblende, quartz, plagioclase, garnet and clinopyroxene result in the formation of plagioclase and pyroxenes (Harlov 2002) with a reduced Aluminium Saturation Index (ASI). It indicates a liquid coexisting with a plagioclase-bearing residual, similar to garnet granulite (Rapp & Watson 1995). Plagioclase is the reaction rate-controlling phase (Johannes & Koepke 2001).

The temperature interval at which a granitic magma starts forming thus indirectly determines its water content. It also separates the 'cold' from the 'hot' magmas (Chappell *et al.* 1998), defining a transition between inheritance-rich and -poor populations of zircons (Miller *et al.* 2003). Hence, low-temperature granites contain restite minerals, often including inherited zircons entrained in the melt. In contrast, high-temperature granites formed from a completely or largely molten magma, in which inherited zircons were not initially present because the melt was not saturated in that mineral (Chappell *et al.* 1998). The incorporation of water in a granitic melt controls the level to which it can ascend in the crust, hence its mobility. It means that during melting, a granitic melt can incorporate a larger fluid phase, provided it results from amphibole, biotite or muscovite breakdown. Hence, the intersection of the solidus for each respective mineral phase with the water-saturated solidus for granites determines the ability of the magma to move from its source region (Fig. 3).

The source region also has consequences for magma composition. Although S-type granites present an obvious crustal component, they are often associated with many mantle-derived enclaves (Barbarin & Didier 1992). Partial melting of K-andesite has been suggested as a source region for generating I-type granites (Roberts & Clemens 1995). However, this model does not fit the isotopic Nd signature of magmas (Castro 2004). A large amount of water should be added to generate melts in enough quantity, since fluid-absent melting of K-rich andesite generates a melt fraction that rarely exceeds 5% (Castro *et al.* 1999). Granodiorite should derive from partial melting of former tonalites (Rapp 1995). A different source region has been suggested for I- and S-type granites (Chappell 1996). However, the ubiquitous observation of granites with transitional features (Patiño Douce 1999) and the lack of experiments that would answer to the source region for I-type granites (Wall *et al.* 1987), make difficult the interpretation of I- and S-type origin. In addition, decoupling between Sr and Nd isotopic studies (Weaver & Tarney 1980; Castro 2004) suggests that many granites, if not all of them, could be of hybrid type, resulting from a mixture from different source regions (Castro *et al.* 1991). A three-source model, including the lower and intermediate crust, plus the underlying mantle, has also been suggested (Collins 1996; Vigneresse 2004). In this scheme, the different types of magma result from a varying percentage of each respective component.

Nevertheless, in those schemes, the underlying mantle essentially controls the melting phase. It provides heat for achieving melting temperature and it can also add enough material fitting the isotopic and chemical composition of granitic melts. However, the length of time required for heat to relax supposes that, in order for melt to be produced in enough volume, segregation of melt requires the same length of time as heat generation. In addition, melting is essentially pervasive within the crust, because the heat transfer is essentially diffusive.

2. Rheological conditions

Whereas melting is essentially looked at in a static mode, the fate of the melt under a given stress field becomes essentially

https://doi.org/10.1017/S0263593300001474 Published online by Cambridge University Press

dynamic. A plastic deforming matrix and melt, incorporating a certain amount of solid phase to become a magma, can no longer respond homogeneously to stress. Rheology of a PMR must first be established before any model of segregation and ascent is suggested.

Despite many models of melt segregation, ascent and emplacement (see reviews in Petford 2003, or in Bons *et al.* 2004), a complete theory for PMR is still required. A reason for this lack is the difficulty of performing experiments under adequately variable strain rates. The long time of relaxation imposed by geological materials requires a rapid deformation; hence it limits investigations to a very restricted domain of strain rate (ε°), around $10^{-4}\,s^{-1}$ for experimental studies. This contrasts with geological strain rates that commonly range from 10^{-10} to $10^{-16}\,s^{-1}$. A different approach to the rheology of PMR considers boundary conditions and the development of instabilities, on the basis of field observations and a series of papers (Vigneresse & Burg 2004) that successively identified the general condition for PMR rheology. Results are briefly reviewed here with their respective implications.

2.1. Mantle versus crust melt extraction

A first point to be addressed is that segregation models valid for mantle material do not apply to the continental crust. The mantle acts as a stress provider to the overlying crust. Hence, convection that develops in the asthenosphere is partly transmitted to the lithosphere, leading to plate displacement. It permanently induces a stress pattern in the continental crust that does not exist to such a level within the oceanic crust. Indeed, the stress level of the lithosphere is partly controlled by the strength of the rigid upper crust. The upper continental crust allows stress of large magnitude to develop, ranging from 100 to 300 MPa for the differential stress. In comparison, the oceanic crust only allows stress values of up to 10 MPa (Yoshinobu & Hirth 2002). The difference in ambient stress level between the two types of plate allows forces to develop that can largely overcome the purely gravitational forces, rendering simple compaction models inadequate for granitic melt extraction.

2.2. Thresholds

The most obvious controlling factor of PMR rheology is the existence of thresholds that separate different domains of behaviour and consequent response to stress. The photo of the partly molten gneiss, taken in a plane perpendicular to the foliation plane (Fig. 2) shows in the upper part of the sample non-connected melt pockets, with consequent no-melt motion. The average percentage of melt is lower than 8%. Conversely, the lower part of the sample, with about 10% melt, shows melt connection and probable motion. Nevertheless, the exact values of such thresholds depend on the rheology contrast between the two phases.

The concept of one unique critical threshold was advanced some time ago (Arzi 1978) though its exact value has long been debated (Renner *et al.* 2000; Rosenberg & Handy 2005). A unique threshold may occur provided the viscosity contrast remains low. In that case the change from a solid- to a liquid-like behaviour is continuous (Fig. 4). It separates two domains and does not give place to instabilities. In contrast, when the viscosity contrast is high, two thresholds determine a transitional state between the two end-members (Fig. 4). This transitional state is a critical state during which instabilities develop (Burg & Vigneresse 2002). It depends on the viscosity contrast between the two phases that varies according to the strain rate (Vigneresse & Burg 2004).

A PMR consists in a mixture of matrix, that deforms plastically, and melt, considered as a Newtonian viscous fluid.

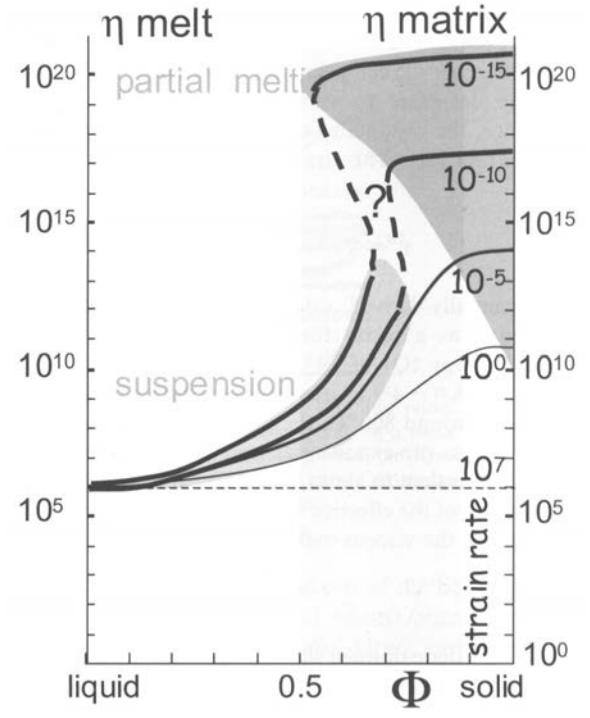

Figure 4 Representation of the viscosity transition between the melt and its matrix under several values of strain rate from 10^{+7} to $10^{15}\,s^{-1}$. For incipient crystal content, the curves in the field of horizontal light grey lines follow the Einstein-Roscoe law (equation 4, see text). With increasing solid content, the curves enter the zone in grey defined in between thresholds. From the other end-member, the curves start from the effective viscosity of the matrix, staying stable within the domain shaded with vertical grey lines. Their bulk shape depends on the strain rate. In case of very rapid deformation, not observable in nature, the contrast between the matrix and the melt could even be null. For fast strain rate, the transition is continuous, yielding to only one threshold, and no instability. In contrast, the large viscosity contrast imposed by the low strain rate results in instabilities development. However, the exact shape of the curve is hardly predictable.

The amount of the two phases is highly variable from place to place and with time, although the bulk respective quantities of each phase can be estimated. With time this amount may vary, generally increasing as a bulk, but it arbitrarily decreases or increases locally, depending on local melt motion. This specificity excludes using any averaging estimate of a bulk viscosity (Ji & Xia 2002). The evolution during melting is not similar to crystallisation (Burg & Vigneresse 2002). Simple thermodynamic consideration indicates that latent heat effects differentiate the two phase transitions (Fig. 4).

A second important point for the transitional state is the general behaviour of each factor. Viscosity (i.e. the inverse ratio of the strain rate response to an applied stress), spatial location and amount of each phase, are essentially non-linear. The combination of several non-linear parameters commonly leads to the development of instabilities (Burg & Vigneresse 2002). The two end-member states for each phase also behave differently. The melt is Newtonian for low strain rates. At 700–900°C, viscosity values are 10^{6}–10^{8} Pa.s for a granitic magma (Clemens & Petford 1999). The melt viscosity diminishes non-linearly when the strain rate becomes faster than $10^{-4.5}\,s^{-1}$ (Webb & Dingwell 1990). However, such a strain rate is not commonly observed in natural situations, since it would correspond to a stress larger than 300 MPa being applied to the magma. Melt also becomes non-Newtonian when the temperature is close to the glass transition (Dingwell *et al.* 1993). In contrast, the matrix deforms plastically. When brought to high temperatures, like those close to melting,

https://doi.org/10.1017/S0263593300001474 Published online by Cambridge University Press

dislocation creep is activated, resulting in a power law of stress (σ) with exponent n=3 (Kohlstedt *et al.* 2000). However, diffusion creep (n=1) can overcome dislocation creep when the strain rate decreases to values lower than $10^{-12}\,s^{-1}$. In consequence, the instantaneous viscosity of the matrix varies with the strain rate. The strain rate ($\varepsilon°$) of the solid matrix writes:

$$\varepsilon° = A\,\sigma^3 \exp(-Q/RT) \quad (2)$$

Experimentally-derived values for plastic deformation of amphibolites, as a proxy for the source rocks, indicate an activation energy (Q) of 243 kJ/mole and a pre-exponential factor of log A = −4·9 (Kirby & Kronenberg 1987). At temperatures of around 800°C, the logarithmic equivalent of the constant terms, pre-exponential and temperature-dependent terms, are equivalent to about −32 (Vigneresse & Burg, 2004). The logarithm of the effective viscosity is thus 10·66–2/3 log $\varepsilon°$

In contrast, the viscous melt deforms linearly:

$$\varepsilon° = \sigma/\eta \quad (3)$$

The intermediate domain shows a different behaviour. For a crystallising magma, the rheology of the liquid with a variable proportion of solid crystals (Φ) is similar to a dilute suspension (Einstein 1906; Roscoe 1952). The viscosity (η) of the dilution departs from its initial value (η_0), i.e. without a solid phase, with a power law that takes into account the interactions within the solid phase:

$$\eta = \eta_0\,(1-\Phi/\Phi_m)^{-n} \quad (4)$$

A commonly adopted exponent for this power law is 2·5 (Lejeune & Richet 1995), decreasing to 1·8 for concentrated suspensions (Krieger & Dougherty 1959) when the interactions between solid particles become preponderant. The viscosity increase due to the solid suspension is about three orders of magnitude when approaching maximum packing Φ_m=0·75 (Vigneresse *et al.* 1996). It defines close packing above which only melt motion is possible. Before that value, a first threshold is observed when the solid particles can transmit stresses, defining a rigidity threshold (Guyon *et al.* 1990). In between, dilatation operates, creating extensional volumes towards which melt is sucked. In contrast, the behaviour during melting is that of the matrix, until a melt film is continuous throughout the source region. This is achieved when the percentage of melt is about 8%, defined as a liquid percolation threshold (Vigneresse *et al.* 1996). The loss of cohesion of the matrix defines the second threshold. In between the two above thresholds for each transition, the situation depends on the contrast between the two end-members. The contrast drastically increases with slower strain rates. In between the curve determined by the Einstein-Roscoe equation and the curve determined by the power law equation for plastic motion of the matrix, the behaviour of the curve cannot yet be directly determined (Fig. 4). Strain partitioning must be considered and a specific rheology for two-phase material must be elaborated.

2.3. Strain partitioning

When two phases coexist and are submitted to stress, strain is partitioned between them, according to their respective viscosity, provided one phase is connected all along the region. Strain partitioning is essential to describe the model, i.e. to separately consider the motion of each phase. Averaging methods, as in the Reuss and Voigt models, respectively consider a geometric and arithmetic average (Guéguen & Palciauskas 1992). The deformation under a common strain rate can be applied to a crystallising magma, featuring the general equation of Herschel-Bulkley (Adler *et al.* 1990). Conversely, a description under a common stress describes the rheology at the onset of melting and it features the general equation for thixotropy (Adler *et al.* 1990; Barnes 1997). In both cases, the rheology of the average medium is non-linear with stress. In fact, averaging methods (Ji & Xia 2002) negate strain partitioning, and thus cannot adequately represent the rheology of a PMR. Hence, during strain partitioning, the stress is transmitted through the strong phase, the corresponding threshold being defined as a rigidity threshold (Guyon *et al.* 1990). Conversely, strain concentrates through the weak phase, here the melt. Strain partitioning also implies that vorticity develops during deformation. It introduces non-coaxial deformation manifested by rotational motion and shear zones. These are ubiquitously present in migmatites (Fig. 5).

Figure 5 Strain partitioning and vorticity in the Chelan migmatites, WA. The melt veins are place where shear and rotation develop due to strain partitioning.

Strain partitions preferentially into the low viscous phase, resulting in a faster motion of the melt compared to its matrix. It manifests through the development of pressure gradients within the matrix that are sinks for the melt. They are aligned within 20° to the direction of shear and are periodically distributed according to the melt percentage (Rosenberg & Handy 2000, 2001; Holtzman *et al.* 2003). The progressive segregation of the melt along sub-parallel veins contributes to the development of anisotropy in the petro-physical properties of the melting region. Assimilating the melting region to a horizontal layer (because the heat progressively diffuses from the heat source) results in a melting front that slowly advances vertically within the crust. With ongoing melting and melt segregation, this horizontal anisotropic melt front starts moving and begins its ascent toward the upper crust, inducing anisotropy in a vertical plane. The two sets of anisotropic rheology are naturally connected and contribute to strain

https://doi.org/10.1017/S0263593300001474 Published online by Cambridge University Press

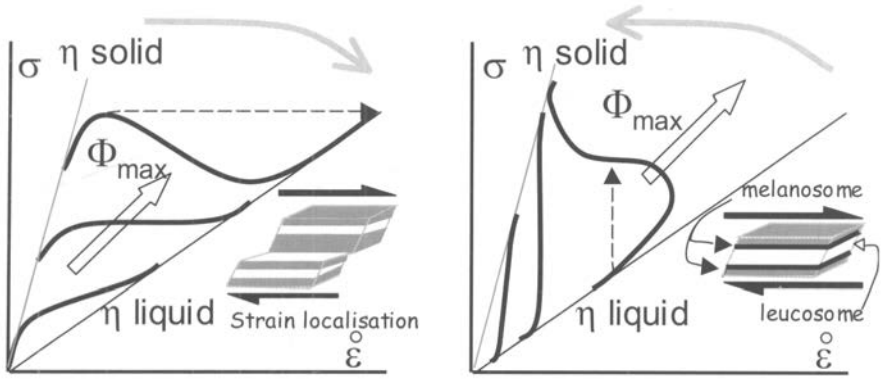

Figure 6 Paths in a bi-logarithmic stress-strain rate diagram, under common stress (on the left) and under common strain rate (on the right) during the transition from the viscosity of a strong phase (solid) to a weak phase (melt) and conversely. Both paths do not involve the same response for a PMR, producing strain partition and localisation in case of a common stress, and phase segregation in case of a common strain rate. Curves are displaced to higher values of stress and strain rate when the maximum packing (Φ_{max}) increases.

partitioning. They also enhance the rotation of the flow lineations (Williams 1990) that occurs preferentially in the weak phase. Progressive uplifting of the melt results, as observed in partitioned transpression (Jones & Tanner 1995; Goodwin & Tikoff 2002; Jones *et al.* 2005).

The partition between strain rate and stress in the two phases depends on the respective paths when the PMR switches from one rheology to the other (Fig. 6). In a bi-logarithmic stress-strain rate diagram, the viscosity plots as lines, with different slopes for the strong and weak phases. Departure to linearity initiates and ends tangentially to each viscosity curve. With increasing contrast between the two viscosity curves, a cusp develops that initiates instability, resulting in metastable solutions. The path for melting, i.e. for going from the strong to the weak phase, takes place under a common stress (Fig. 6). In contrast, the path develops along a common strain rate when the transition is from the weak to the strong one, i.e. for crystallisation (Fig. 6). Facing such instabilities, the system locally responds by feedback loops (Burg & Vigneresse 2002) and changes operate at all scales, from melt films along grain boundaries to melt segregation within the crust. They lead to strain localisation in the case of a common stress regime (Fig. 6). Conversely, phase separation and crystal sorting develop under a common strain rate (Olmsted 1999; Vigneresse & Burg 2004). Such effects, manifested by magma banding and shear localisation, are ubiquitous in field observations on PMR.

2.4. PMR rheology and strain rate dependence

A full 3-D diagram taking into account the strain rate remains to be constructed from the respective behaviour and the amount of each phase (Vigneresse & Burg 2004). It should concentrate on the transitional state previously identified and it should justify the shape of the curves in Figure 4. The previous 2-D diagrams commonly suggested (Arzi 1978; Renner *et al.* 2000; Rosenberg & Handy 2005), show viscosity variation as a function of the solid phase. They have been built independently of the strain rate. Those diagrams may be correct to represent a transition at a given strain rate, i.e. a given viscosity contrast. They are obviously false for a varying effective viscosity of one phase.

In PMR, the viscosity of the weak phase is usually lower than that of the strong phase. However, the contrast could be null for a very fast strain rate (Fig. 4), and for a still faster strain rate, the melt could be the strong phase. Such a strange situation occurs in saturated sand when strongly shacked during earthquake, leading to soil liquefaction (Ishihara 1993; Vigneresse 2004). Under such fast strain rates, the saturated sand behaves as a single-phase body, vibrating up to large amplitudes, and sand is expelled out of the liquid, as in mud volcanoes. Soil liquefaction and related phenomena are responsible for tremendous damage during earthquakes (Ishihara 1993).

In the case of granitic magma generation, the viscosity contrast between the matrix and melt remains in the range of 10^9 to 10^{13} (Burg & Vigneresse 2002). The viscosity contrast is the lowest at high strain rate and becomes null for a value of $10^{+7}\,s^{-1}$. Hopefully, this case does not develop for PMR in nature. The contrast increases with decreasing strain rate. Experimental studies are realised under strain rates of about 10^{-4} to $10^{-5}\,s^{-1}$ (Rutter & Neuman 1995). The matrix presents an effective viscosity of the order of 10^{14} Pa.s, resulting in a viscosity contrast of 10^8 with the melt. The transition between the two end-members is continuous, with a sigmoidal shape (Fig. 4). For slow strain rate ($10^{-15}\,s^{-1}$), as it occurs during magma emplacement and crystallisation, the effective viscosity of the matrix is 10^{17} Pa.s, resulting in a viscosity contrast of 10^{11}. However, slow strain rate also implies a longer relaxation time for each phase, allowing reorganisation of the system. Consequently, the stability domain corresponding to each of the two end-members is extended, resulting in an overlap of those domains. Such situations are intrinsically unstable, and the rheology adopts that of either the strong or the weak phase. The curve joining the two end-members must adopt a cusp shape (Fig. 4), with the internal part of the cusp never observed in natural situation.

A total 3-D diagram, not obtained from considerations about catastrophes (Thom 1980), is constructed from the rheology of the end-members. The transitional state presents a cusp shape resulting from the combination of a power law for stress (n=3) and a linear rheology (n=1), yielding a cubic equation. Indeed, the total energy of the mixture is the sum of each product of respective strain by the applied stress. The power equation is the sum of respective products of strain rate by stress, corresponding to a degree four equation in stress. Equilibrium condition requires that the derivative of the power is minimum, leading to a cubic equation in terms of stress. Depending on the boundary conditions, the cubic equation presents one or three roots, presenting a cusp shape and metastable solutions (Fig. 4) (Vigneresse & Burg 2004).

The existence of metastable solutions is also suggested after a simple transformation of the cubic surface of a 3-D diagram into several 2-D diagrams depending on the strain rate (Fig. 7). The negative logarithm of the viscosity is plotted as a function of the solid content (Φ), indicating the inverse of the viscosity

https://doi.org/10.1017/S0263593300001474 Published online by Cambridge University Press

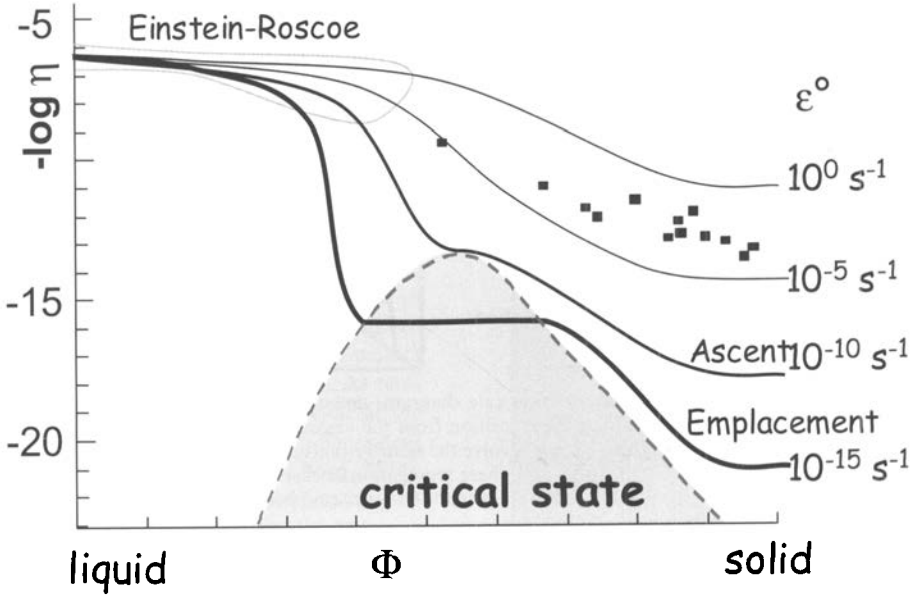

Figure 7 Critical state development during the transition liquid-solid in PMR. The melt-dominated behaviour follows the Einstein-Roscoe law for a low solid content (domain with horizontal grey lines). At the other end of the diagram, the matrix presents a power law for stress, and its effective viscosity depends on the strain rate. The critical region is the place where instabilities develop, represented with grey shading. Experimental data of PMR deformation (Rutter & Neumann 1995) have been posted as black squares. The fields of strain rate developed during ascent and emplacement of granitic magmas are represented in grey.

as a function of the solid phase. The curves are plotted for a given strain rate. Each curve starts from a constant value for the melt, but ends with decreasing values for the matrix. A viscosity value of 10^6 Pa.s is assumed for a granodiorite melt, but it can be different to accommodate chemical variations of the starting melt (Clemens & Petford 1999). The progressive increase of the solid phase is modelled with the Einstein–Roscoe equation. It corresponds to an increase of the viscosity by about three orders of magnitude. At the other end, effective viscosity values for plastic amphibolites are used for representing the matrix. The values stand constant as long as a certain amount of liquid is not present to assure melt connection. For fast strain rates, the curves from the two end members can be easily connected together. In contrast, for low strain rates, the curve passes through an interval during which no definite value can be assigned to the mixture. It defines a critical zone in which instabilities develop. The diagram (Fig. 7) is quite similar to phase diagrams used for fluid activities, as for instance pressure and volumes diagrams as a function of temperature. The critical curve corresponds to the values of the thresholds that determine instability development. When experimental data (Rutter & Neumann 1995) are plotted within this diagram, they plot perfectly on curves defined for fast strain rates (10^4 to 10^5 s^{-1}). The very fast strain rates imposed by the experiments do not enter into the critical state, thus masking the development of instabilities.

3. Modelling melt segregation and ascent

The previous findings have been incorporated into numerical models of melt segregation. They have also been checked with analogue experiments. The two types of numerical descriptions allowed identification of the controlling parameters of melt segregation.

The numerical model is the usual Eulerian description, involving the equations for mass and moment conservation for both the melt and its matrix (Rabinowicz & Vigneresse 2004). It differs from previous models (McKenzie 1984; Stevenson 1989) since it takes into account pure and simple shear deformation. The results, scaled in time and length, are compared *a posteriori* with field observations. They are used to check the validity of the model according to its input parameters. In contrast, the second type of representation uses a Lagrangian description, through a cellular automaton (Vigneresse & Burg 2000, 2005). Melt motion under pure and/or simple shear, is estimated from the point of view of the melt from melt cell to another cell. Rules imply threshold values that allow melt motion or melt escape. The model is stationary, assuming an infinite source and sink for the melt. Results cannot provide a geometric description for melt segregation, but allow identification of the leading parameters controlling melt segregation. Those numerical models favourably compare with a similar analogue approach using the progressive melting of a plastic deforming material (Barraud *et al.* 2001, 2004) and wheat fermentation (Bons *et al.* 2001, 2004). In contrast, small-scale analogue models provide the geometry for melt segregation (Rosenberg & Handy 2000, 2001).

3.1. Results of the numerical models

An important qualitative result from those models is that the controlling factors for melt segregation are few. They are the applied stress pattern, namely pure and/or simple shear, the amount of melt, the viscosity contrast between the two phases, and by consequence the strain rate. The amount of heat also controls the viscosity contrast by changing the viscosity of the matrix and the available melt content. The time for all those processes to develop is a limiting factor imposed by natural observations on strain rate and pluton construction rate.

The numerical models demonstrate that melt segregation is discontinuous in time and space. Segregation starts at any moment of the process. This is also observed in analogue models (Walte *et al.* 2005). Melt segregation strongly depends on a restricted window for the values of the input parameters and boundary conditions. Compaction (McKenzie 1984; Stevenson 1989) results in the development of compaction bands in which melt segregates. The spacing is periodic (Rabinowicz *et al.* 2001) with a wavelength (λ) that depends on

https://doi.org/10.1017/S0263593300001474 Published online by Cambridge University Press

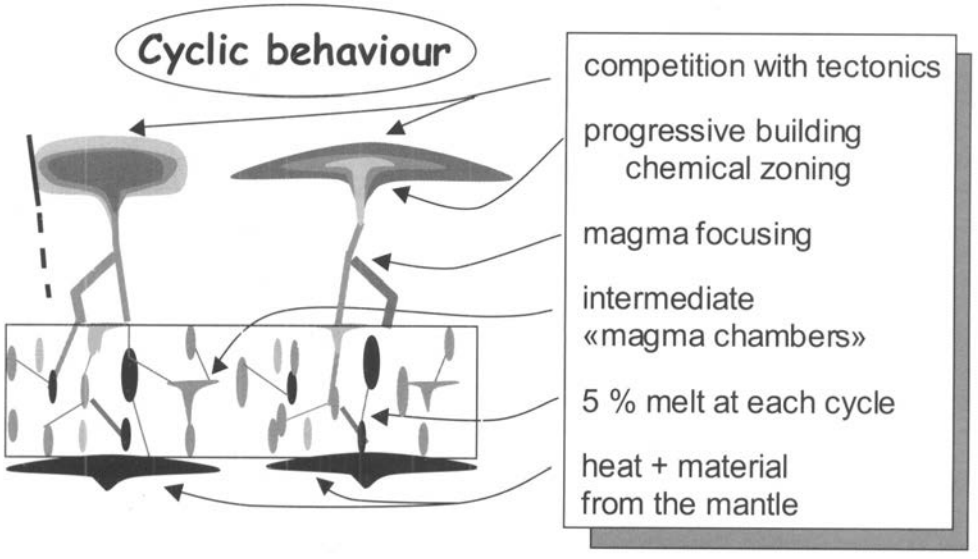

Figure 8 Major implications of the m(M-SAE) model, pointing out the effects a discontinuous segregation, ascent and emplacement of magma may have on the construction of a granitic pluton.

the ratio of the viscosity between matrix (η_M) and melt (η_m), the permeability (k) and the amount of melt ($\varphi = 1 - \Phi$)

$$\lambda = (\eta_M/\eta_m)^{1/2}\,(k/\varphi)^{1/2} \qquad (5)$$

In this equation, the viscosity ratio is experimentally determined at 10^{13}, as well as the permeability of the lower crust (10^{-15} m^2), that depends on the grain size (Maaløe & Scheie 1982). Compaction models, i.e. with purely gravitational forces, that perfectly apply to mantle conditions (McKenzie 1984; Stevenson 1989), are inadequate when applied to melt segregation within the continental crust (Brown *et al.* 1995) because they require too long a time (20 My) before vein spacing reaches a metric order (Rabinowicz & Vigneresse 2004). Additional forces should be added to gravity. This is possible because the continental crust is strong enough to sustain larger stress amplitudes. Adding pure and simple shear causes widespread melt segregation, even in the case of low-viscosity melts, as for instance for very wet granites. In this case convection leads to the formation of stromatic structures, a state that could also be reached only with a very large melting rate, leading to matrix cohesion loss (Brown *et al.* 1995). Simple shear is the additional force that helps to displace the melt in between compaction bands without altering the spacing between bands (Rabinowicz & Vigneresse 2004). Non-coaxial deformation is ubiquitously observed in migmatites (Fig. 5).

The restricted window for the input parameters to match time and space scaling also applies to melt fraction. Numerical results consider that melt is connected, though this depends on the scale of observation. However, the bulk degree of melting should range between 5% and 10% for each volume of segregated melt.

The total degree of melting has indirect consequences on the viscosity values of both melt and matrix. Indeed, the first-produced melts present the highest water content, hence the lowest viscosity. More melting implies less water in the melt, increasing the melt viscosity. This effect adds to the reduced water content of the evolving magma (Fig. 3). However, the change in water content in the melt also implies a change in the rheology of the matrix evolving from a wet amphibolite to a dry granulite. A factor of ten is estimated when melt increases by 5% (Rabinowicz & Vigneresse 2004). Nevertheless, the change in melt viscosity is compensated by the change in composition of the matrix, so that the two effects balance each other. Hence, the viscosity contrast remains constant on a first order.

The intensity of the strain rate is partly controlled by the width of the shear zone. The wider the shear zone, the slower should be the strain rate. For a given increase in the amount of melt (5%), the time necessary for both compaction and shear increases by about one order of magnitude, provided the strain rate, i.e. the width of the shear zone, remains the same. However, it decreases by four orders of magnitude when strain rate under simple shear decreases by about four orders of magnitude. Finally, for too low strain rates (10^{-10} s^{-1}) the width of the shear zone and the time required for segregation do not correspond to those observed during granite generation.

3.2. Melt focusing during the ascent

The viscosity variation between the melt and its surrounding varies from the source region to the emplacement region. It consequently changes the compaction length (equation 5). Hence the permeability of the upper to intermediate crust varies, as well as the effective viscosity of the crust. Assuming a permeability value of 10^{-11} m^2 (Ingebritsen & Manning 1999), large magma conduits and a spacing of 50 km between plutons result in a viscosity estimate of 10^{21} Pa.s, providing the melt content is fixed at 10% with a viscosity of 10^5 Pa.s. The corresponding viscosity agrees with similar values for the continental crust.

4. Discussions and implications

Discontinuous segregation and ascent of magma have important consequences on the process of building a granitic pluton. They lead to the possibility of having intermediate magma chambers with different temperature and magma composition. They have obvious implications on the mechanisms of creating space for pluton intrusions (Fig. 8).

4.1. Intermediate magma chambers and magma mixing

Isotopic and geochemical discontinuities indicate that not all facies are the result of the chemical evolution of a unique blob of magma as a closed system (Cashman & Bergantz 1991). Too large isotopic differences are commonly interpreted as the

https://doi.org/10.1017/S0263593300001474 Published online by Cambridge University Press

result of mixing between different source regions. However, it seems difficult to involve contrasted chemical contributions from different regions of the mantle.

A discontinuous magma segregation and extraction leads to the possibility of having intermediate magma chambers of any size, located and staying close to the source region for various times. They may evolve differently, depending on their initial composition, hence internal temperature and the region in which they accumulate. A progressive assimilation or contamination from the surrounding material is always possible. In that scheme, an intermediate magma chamber is a collection of mushy dykes more or less interconnected. It is the best place to develop internal advection, since they can be considered as formed by mostly liquid magmas, with some restitic bodies. These can be rapidly assimilated by back reactions (Beard *et al.* 2005). The low viscosity of the mostly liquid magma, within a loosely organised matrix, facilitates the mixing, through constantly reorganising walls subjected to external stresses. This would develop vigorous strain in the magma chamber that would generate mixing and chemical homogenisation.

Magma mixing in high-level magma chambers is unlikely, owing to the high viscosity of the granitic magmas, maybe with the exception of hot alkaline magmas. Hence, large forces are required to adequately mix magmas. Successive inputs of magma with variable composition and temperature certainly induce temperature, density and viscosity gradients. However, the largest contrast could occur when liquid basalt at about 1200 °C intrudes a 600 °C crystallising granite. Thus a contrast of 600 °C is assumed with a viscosity contrast of about 10^7 Pa.s and a 200 kg/km^3 for the density contrast. A rapid computation of Rayleigh numbers indicates that the critical length values for convection are reached at about 5 m. This is about the scale of convective structures observed in plutons (Weinberg *et al.* 2001). Magma mixing is therefore unlikely on a larger scale (> km) in high-level magma chambers. However, mixing is certainly feasible in deeper reservoirs, when the temperature difference between magmas is reduced, with higher average value, enhancing diffusion exchange in addition to convection. It implies that most magmas are hybrid (Castro *et al.* 1991).

4.2. Discontinuous magma outputs

Successive magma pulses are necessary to build a granitic pluton. Hence, various petrological and mineral facies have long been described that form a single pluton. The interpretation of their variety has often been attributed to internal fractionation and magma differentiation. However, arguments have been proposed that do not match such a continuous evolution (Roberts & Clemens 1995).

Mineral fabrics document discontinuities between adjacent facies (review in Bouchez 1997). They would correspond to several pulses of magma, each recording a specific period of emplacement. Their non-alignment, the orientation of which can sometimes be highly discordant, shows that the flow has not always been continuous. The observation of petrographic facies showing sharp boundaries also documents a temperature interval during the crystallisation of the magma between adjacent facies. It corroborates the presence of detached blocs of one facies in another, without any evidence of crystallisation history between them.

Discontinuous magma inputs essentially mark through discordant contacts, that is when the time interval between pulses is large enough to provide contrasted fabrics, or when the composition of the magma differs significantly. In some cases, the mineralogy abruptly changes, evolving from a biotite-dominant to a muscovite-rich facies, for instance. In other cases, the mineralogy remains similar, but the grain size varies, passing from coarse to fine grains. Differences in orientation between magmatic fabrics record changes in incremental strain. Age determination for successive intrusions is feasible (Coleman *et al.* 2004), although actually problematic, since the time lag between intrusions is often within the resolution range of geochronology methods.

Mineralogical zoning resulting in normal (Allen 1992; Stephens 1992) or reversed (Ayuso 1984; Bourne & Danis 1987) zoned plutons proceeds from a similar history. Whether or not magma has time to partly crystallise depends on the time interval between magma inputs. Two cases are possible for the new magma, commonly more evolved chemically. In case of rapid intrusions, the new magma intrudes the former, not yet crystallised, magma because it offers the least resistance, resulting in normal zoning. In case of longer delay between magma pulses, the former magma may be solidified and the new magma must take place at the rim of the former, giving rise to reverse zoning (Hecht & Vigneresse 1999).

4.3. Pluton building and crustal relaxation

For a long time, the formation of granitic plutons has been described in terms of space. Indeed, the instantaneous creation of volume in which magma could take place in the upper crust had long been known as the 'room problem' (Read 1957). This had partly been solved by changing the boundary conditions, i.e. by uplifting the roof (Pollard & Muller 1976), or by depressing the floor (Cruden 1998), or by involving the tectonic creation of space that would be filled by the magma (Hutton 1982; Guineberteau *et al.* 1987).

Repeated discontinuous inputs of magma partly solve the room problem, since the crust has time to relax between magma pulses. Given that the roots of a pluton are close to the brittle/ductile transition (Vigneresse 2004), the relaxation (τ_r) time of the crust can be approximated as a function of its bulk viscosity (η) and elastic shear modulus (G)

$$\tau_r = \eta/G \qquad (6)$$

Given the value of 10^{21} Pa.s for the effective viscosity of the mid crust and about 5 10^{10} N/m^2 for the elastic modulus, it takes about 16 ky for the crust to relax, which is less than the estimated time interval (about 30 ky) between magma pulses (Glazner *et al.* 2004).

The global shape of granitic plutons documents another aspect of growth through successive magma pulses. Hence, the 3-D shape of plutons, interpreted from gravity surveys, shows that the majority of massifs present a flat-floored shape (Vigneresse *et al.* 1999). Conversely, other massifs show a deeper floor, with steep walls, indicating a wedge shape. The walls of those massifs are generally tectonically controlled. The dichotomy in shape is reinforced when plotted in a Flinn-like diagram (Flinn 1962) describing the shape of strain ellipsoids. Length is assimilated to the largest quantity, followed by width and thickness. The diagram describes the ratio of the length to the width (L/W) versus the ratio of the width to the thickness (W/T). Relative to deformation, a plane strain line separates constriction from flattening domains. When plotted on this diagram, the wedge shape plutons plot with the constriction field, whilst flat-floored plutons are within the flattening domain (Fig. 9). The self-affine variations of volume for laccoliths (McCaffrey & Petford 1997) and plutons (Petford *et al.* 2000) are also plotted for comparison. The two curves have been computed from the equations provided by the authors, with arbitrary values of dimensions ranging from 1 to 50 km for the width (Fig. 9).

The wedge shape massifs correspond to a tectonic-dominated stress pattern (Hogan *et al.* 1995; Vigneresse *et al.*

https://doi.org/10.1017/S0263593300001474 Published online by Cambridge University Press

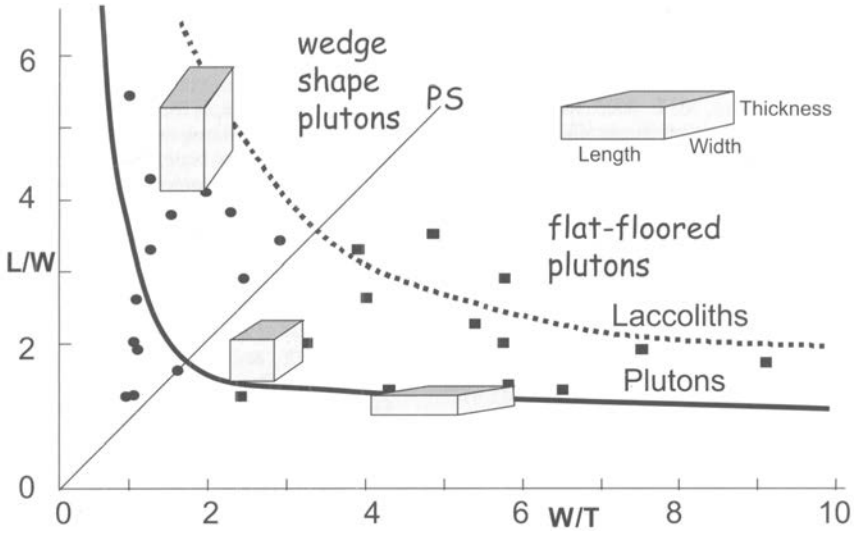

Figure 9 Flinn diagram, showing the respective ratio L/W versus W/T, the respective length, width and thickness of a granitic pluton. Two fields are distinguished for plutons with a wedge shape and those flat-floored. Self-affine curves relating the length and width of laccoliths and plutons respectively (McCaffrey & Petford 1997; Petford *et al.* 2000) are also plotted. They have been computed, assuming one dimension of the body varying between 1 and 50 km. Most wedge shape granitic bodies are in the constriction field, whilst flat-floored massifs are in the flattening domain.

1999). Conversely, when the internal magma pressure dominates the external stress field, the massifs adopt a flat-floored shape, expanding laterally since it cannot ascend any more. Thus the two domains of the Flinn-like diagram (Fig. 9) indicate the competition between magma ascent followed by lateral magma expansion and tectonic forces that help in creating room for the magma.

4.4. Magmatism and tectonism

The last point under discussion relates to the long-standing observation that links magmatism to tectonics (Pitcher 1993). Indeed both are intimately linked up to the point that orogenic cycles can be viewed as a competition between those two ways of dissipating energy (Burg 1999). Magmatism relates to heat source whereas tectonics is a direct manifestation of stress intensity. Depending on their respective contribution, an orogenic cycle could give place to widespread deformation, as for instance the PanAfrican-Brasiliano, circa 600 Ma (Neves *et al.* 1996) or to intense magmatism that gave place to numerous pluton emplacements as in West Africa at about 2·1 Ga (Pons *et al.* 1995).

5. Conclusions

A new scheme for granite generation is presented that considers the mantle participation before melting, and then segregation, ascent and emplacement of magma, giving place to the m(M-SAE) model. Whilst melting is essentially continuous with time, the last three states occur discontinuously, owing to the non-linear character of PMR rheology, melt distribution and its amount, as well as to strain partitioning between the two phases, namely melt and its matrix. Thresholds controlling melt motion and matrix loss of cohesion bracket the non-linear and discontinuous segregation. As a result, intermediate magma chambers can develop. A granitic pluton is therefore built from successive bursts of magma with different temperature and composition. The time interval between magma pulses leaves time for the surrounding crust to relax. The bulk shape of the pluton also results from the competition between the magma internal pressure and the external stress field.

6. Acknowledgments

It is a great pleasure and honour to participate in a volume honouring Wally Pitcher. I presented the first contribution about the 3-D shape at depth of granitic plutons in 1990 in a meeting honouring Wally's retirement. Since that time, he always encouraged me to apply physical notions to the understanding of field observations. They remain the basis of our perception. Thanks also to the numerous people who participated to the elaboration of this new paradigm for granite generation. They include people from experimental labs, analogue and numerical modellers, field geologists, as well as theoretical investigators. Constructive comments were provided by P. Barbey and C. Rosenberg, and by N. Petford, A. Cruden and B. Bonin during the review. P. Lagrange (CREGU) is acknowledged for the figures.

7. References

Adler, P., Nadim, A. & Brenner, H. 1990. Rheological models of suspensions. *Advances in Chemical Engineering* **15**, 1–67.

Allen, C. M. 1992. A nested diapir model for the reversely zoned Turtle Pluton, southeastern California. *Transactions of the Royal Society of Edinburgh: Earth Sciences* **83**, 179–90.

Annen, C. & Sparks, R. S. J. 2002. Effects of repetitive emplacement of basaltic intrusions on thermal evolution and melt generation in the crust. *Earth and Planetary Science Letters* **203**, 937–55.

Arzi, A. A. 1978. Critical phenomena in the rheology of partially melted rocks. *Tectonophysics* **44**, 173–84.

Ayuso, R. A. 1984. Field relations, crystallization and petrology of reversely zoned granitic plutons in the Bottle Lake complex, Maine. *USGS Professional Paper* **1320**, 1–58.

Bacon, C. R. 1986. Magmatic inclusions in silicic and intermediate volcanic-rocks. *Journal of Geophysical Research* B91, 6091–112.

Barbarin, B. & Didier, J. 1992. Genesis and evolution of mafic microgranular enclaves through various types of interaction between coexisting felsic and mafic magmas. *Transactions of the Royal Society of Edinburgh: Earth Sciences* **83**, 145–53.

Barnes, H. A. 1997. Thixotropy – A review. *Journal of Non Newtonian Fluid Mechanics* **70**, 1–33.

Barraud, J., Gardien, V., Allemand, P. & Grandjean, P. 2001. Analog modelling of melt segregation and migration during deformation. *Physics and Chemistry of the Earth* **A26**, 317–23.

Barraud, J., Gardien, V., Allemand, P. & Grandjean, P. 2004. Analogue models of melt-flow networks in folding migmatites. *Journal of Structural Geology* **26**, 307–24.

https://doi.org/10.1017/S0263593300001474 Published online by Cambridge University Press

Bauer, P., Rosenberg, C. L. & Handy, M. R. 2000. 'See-through' deformation experiments on brittle–viscous norcamphor at controlled temperature, strain rate and applied confining pressure. *Journal of Structural Geology* **22**, 281–9.

Beard, J. S., Ragland, P. C. & Crawford, M. L. 2005. Reactive bulk assimilation: A model for crust-mantle mixing in silicic magmas. *Geology* **33**, 681–4.

Bergantz, G. W. 1989. Underplating and partial melting: Implications for melt generation and extraction. *Science* **245**, 1093–5.

Bons, P. D., Dougherty-Page, J. & Elburg, M. A. 2001. Stepwise accumulation and ascent of magmas. *Journal of Metamorphic Geology* **19**, 627–33.

Bons, P. D., Arnold, J., Elburg, M. A., Kalda, J., Soesoo, A. & van Milligen, B. P. 2004. Melt extraction and accumulation from partially molten rocks. *Lithos* **78**, 25–42.

Bouchez, J. L. 1997. Granite is never isotropic: an introduction to AMS studies of granitic rocks. *In* Bouchez, J. L., Hutton, D. H. W. & Stephens, W. E. (eds) *Granite: from Segregation of Melt to Emplacement Fabrics*, 95–112. Dordrecht: Kluwer Academic Publishers.

Bourne, J. & Danis D. 1987. A proposed model for the formation of reversely zoned plutons based on a study of the Lacorne complex, Superior Province, Quebec. Canadian *Journal of Earth Sciences* **24**, 2506–20.

Brown, M., Averkin, Y. A., McLellan, E. L. & Sawyer, E. W. 1995. Melt segregation in migmatites. *Journal of Geophysical Research* **B100**, 15655–80.

Burg, J. P. & Vigneresse, J. L. 2002. Non-linear feedback loops in the rheology of cooling-crystallising felsic magma and heating-melting felsic rock. *In* De Meer, S., Drury, M. R., De Bresser, J. H. P. & Pennock, G. M. (eds) *Deformation Mechanisms, Rheology and Tectonics: Current Status and Future Perspectives. Geological Society, London, Special Publication* **200**, 275–92.

Burg, J. P. 1999. Ductile structures and instabilities: their implication for Variscan tectonics in the Ardennes. *Tectonophysics* **309**, 1–25.

Cashman, K. V. & Bergantz, G. W. 1991. Magmatic processes. *Reviews of Geophysics* **29**, 500–12.

Castro, A. 2004. The source of granites: inferences from the Lewisian complex. *Scottish Journal of Geology* **40**, 49–65.

Castro, A., Moreno Ventas, I. & De la Rosa, J. 1991. H-type (hybrid) granitoids: a proposed revision of the granite type classification. *Earth Science Reviews* **31**, 237–53.

Castro, A., Corretgé, L. G., El-Biad, M., El-Hmidi, H., Fernadez, C. & Patiño Douce, A. E. 1999. Experimental constraints on Hercynian anatexis in the Iberian Massif, Spain. *Journal of Petrology* **41**, 1471–88.

Chappell, B. W. 1996. Compositional variation within granite suites of the Lachlan Fold Belt: its causes and implications for the physical state of granite magma. *Transactions of the Royal Society of Edinburgh: Earth Sciences* **87**, 159–70.

Chappell, B. W., White, A. J. R. & Wyborn, D. 1987. The importance of residual source material (restite) in granite petrogenesis. *Journal of Petrology* **28**, 1111–38.

Chappell, B. W., Bryant, C. J., Wyborn, D., White, A. J. R. & Williams, I. S. 1998. High and low-temperature I-type granites. *Resource Geology* **48**, 225–35.

Chappell, B. W. & White, A. J. R. 2001. Two contrasting granite types: 25 years later. *Australian Journal of Earth Sciences* **48**, 489–99.

Clemens, J. D. 1990. The granulite – granite connexion. *In* Vielzeuf, D. & Vidal, P. (eds) *Granulite and Crustal Evolution.* NATO ASI series **C311**, 25–36. Dordrecht: Kluwer Academic Publishers.

Clemens, J. D. & Petford, N. 1999. Granitic melt viscosity and silicic magma dynamics in contrasting tectonic settings. *Journal of the Geological Society, London* **156**, 1057–60.

Coleman, D. S., Gray, W. & Glazner, A. F. 2004. Rethinking the emplacement and evolution of zoned plutons: Geochronologic evidence for incremental assembly of the Tuolumne Intrusive Suite, California. *Geology* **32**, 433–6.

Collins, W. J. 1996. Lachlan Fold Belt granitoids: products of three-component mixing. *Transactions of the Royal Society of Edinburgh: Earth Sciences* **87**, 171–81.

Crank, J. 1975. *The Mathematics of Diffusion.* Oxford: Oxford University Press.

Cruden, A. R. 1998. On the emplacement of tabular granites. *Journal of the Geological Society, London* **155**, 853–62.

Dingwell, D. B., Bagdassarov, N. S., Bussod, N. S. & Webb, S. L. 1993. Magma rheology. *In* Luth, R. W. (ed.) *Experiments at High Pressure and Applications to the Earth's Mantle*, 131–96. Nepean, Ontario: Mineralogical Association of Canada.

Einstein, A. 1906. Eine neue Bestimmung der Molekul-dimensionnen. *Annales de Physique* **19**, 289–306.

Flinn, D. 1962. On folding during three-dimensional progressive deformation. *Quarterly Journal of the Geological Society of London* **118**, 385–433.

Furman, T. & Spera, F. J. 1985. Co-mingling of acid and basic magma with implications for the origin of mafic I-type xenoliths: field and petrochemical relations of an unusual dike complex at Eagle Lake, Sequoia National Park, California, USA. *Journal of Volcanology and Geothermal Resources* **24**, 151–78.

Glazner, A. F., Bartley, J. M., Coleman, D. S., Gray, W. & Taylor, R. Z. 2004. Are plutons assembled over millions of years by amalgamation from small magma chambers? *GSA Today* **14**, 4–11.

Goodwin, L. B. & Tikoff, B. 2002. Competency contrast, kinematics, and the development of foliations and lineations in the crust. *Journal of Structural Geology* **24**, 1065–85.

Guéguen, Y. & Palciauskas V. 1992. *Introduction à la Physique des Roches.* Paris: Hermann.

Guineberteau, B., Bouchez, J. L. & Vigneresse, J. L. 1987. The Mortagne granite pluton (France) emplaced by pull apart along a shear zone: structural and gravimetric arguments and regional implication. *Geological Society of American Bulletin* **99**, 763–70.

Guyon, E., Roux, S., Hansen, A., Bideau, D., Troadec, J. P. & Crapo. H. 1990. Non-local and non-linear problems in the mechanics of disordered systems: application to granular media and rigidity problems. *Reports on Progress in Physics* **53**, 373–419.

Harlov, D. E. 2002. Review of petrographic and mineralogical evidence for fluid induced dehydration of amphibolite facies to granulite facies rocks. *Zeitschrift für Geologische Wissenschaften* **30**, 13–36.

Harris, N., Ayers, M. & Massey, J. 1995. Geochemistry of granitic melts produced during incongruent melting of muscovite: implications for the extraction of Himalayan leucogranite magmas. *Journal of Geophysical Research* **B100**, 15767–77.

Hecht, L. & Vigneresse, J. L. 1999. A multidisciplinary approach combining geochemical, gravity and structural data: implications for pluton emplacement and zonation. *In* Castro, A., Fernandez. C. Vigneresse, J. L. (eds) *Understanding Ggranites: Integrating New and Classical Techniques. Geological Society, London, Special Publication* **168**, 95–110.

Hildreth, E. W. & Moorbath, S. 1988. Crustal contributions to arc magmatism in the Andes of Central Chile. *Contributions to Mineralogy and Petrology* **76**, 177–95.

Hogan, J. P. & Gilbert, M. C. 1995. The A-type Mount Scott Granite sheet: Importance of crustal magma traps. *Journal of Geophysical Research* **B100**, 15779–92.

Holtzman, B. K., Kohlstedt, D. L., Zimmerman, M. E., Heidelbach, F., Hiraga, T. & Hustoft, J. 2003. Melt segregation and strain partitioning: implications for seismic anisotropy and mantle flow. *Science* **301**, 1227–30.

Hutton, D. H. W. 1982, A tectonic model for the emplacement of the main Donegal granite, NW Ireland. *Journal of the Geological Society London* **139**, 615–31.

Ingebritsen, S. E. & Manning, C. E. 1999. Geological implications of a permeability-depth curve for the continental crust. *Geology* **27**, 1107–10.

Ishihara, K. 1993. Liquefaction and flow failure during earthquakes. *Géotechnique* **43**, 351–415.

Ji, S. C. & Xia, B. 2002. *Rheology of Polyphase Earth Materials* Montreal: Polytechnic International Press.

Johannes, W. & Koepke, J. 2001. Incomplete reaction of plagioclase in experimental dehydration melting of amphibole. *Australian Journal of Earth Sciences* **48**, 581–90.

Jones, R. R., Holdsworth, R. E., McCaffrey, K. J. W., Clegg, P. & Tavarnelli, E. 2005. Scale dependence, strain compatibility and heterogeneity of three-dimensional deformation during mountain building: a discussion. *Journal of Structural Geology* **27**, 1190–204.

Jones, R. R. & Tanner, P. W. G. 1995. Strain partitioning in transpression zones. *Journal of Structural Geology* **17**, 793–802.

Kirby, S. H. & Kronenberg, A. K. 1987. Rheology of the lithosphere: Selected topics. *Reviews of Geophysics* **25**, 1219–44.

Kohlstedt, D. L., Bai, Q, Wand, Z. C. & Mei, S. 2000. Rheology of partially molten rocks. *In* Bagdassarov, N., Laporte, D. & Thompson, A.B. (eds) *Physics and Chemistry of Partially Molten Rocks*, 3–28. Dordrecht: Kluwer Academic Publishers.

Krieger, I. M. & Dougherty, T. J. 1959. A mechanism for non-Newtonian flow in suspensions of rigid spheres. *Transactions of the Society of Rheology* **3**, 137–52.

Lejeune, A. M. & Richet, P. 1995. Rheology of crystal-bearing silicate melts: an experimental study of high viscosities. *Journal of Geophysical Research* **B100**, 4215–29.

Maaløe, S. & Scheie, A. 1982. The permeability controlled accumulation of primary magma. *Contributions to Mineralogy and Petrology* **81**, 350–7.

Martin, R. F. & Piwinskii, A. J. 1972. Magmatism and tectonic setting. *Journal of Geophysical Research* **77**, 4966–75.

McCaffrey, K. J. W. & Petford, N. 1997. Are granitic intrusions scale invariant? *Journal of the Geological Society, London* **154**, 1–4.

McKenzie, D. 1984. The generation and compaction of partially molten rock. *Journal of Petrology* **25**, 713–65.

Menhert, K. R. 1968. *Migmatites and the Origin of Granitic Rocks.* Amsterdam: Elsevier.

Miller, C. F., Meschter McDowell, S. & Mapes, R. W. 2003. Hot and cold granites? Implications of zircon saturation temperatures and preservation of inheritance. *Geology* **31**, 529–32.

Neves, S. P., Vauchez, A. & Archanjo, C. J. 1996. Shear zone-controlled magma emplacement or magma-assisted nucleation of shear zones? Insights from northeast Brazil. *Tectonophysics* **262**, 349–64.

Olmsted, P. D. 1999. Two-state shear diagrams for complex fluids in shear flow. *Europhysics Letters* **48**, 339–45.

Patiño Douce, A. E. 1999. What do experiments tell us about the relative contributions of crust and mantle to the origin of granitic magmas. *In* Castro, A., Fernandez, C. & Vigneresse, J. L. (eds) *Understanding granites: Integrating New and Classical techniques. Geological Society, London, Special Publication* **168**, 55–75.

Patiño Douce, A. E. & Beard, J. S. 1995. Dehydration melting of biotite gneiss and quartz amphibolite from 3 to 15 kbar. *Journal of Petrology* **96**, 707–38.

Patiño Douce, A. E. & Harris, N. 1998. Experimental constraints on Himalayan anatexis. *Journal of Petrology* **39**, 689–710.

Patiño Douce, A. E. & Johnston, A. D. 1991. Phase equilibria and melt productivity in the pelitic system: implications for the origin of peraluminous granitoids and aluminous silicates. *Contributions to Mineralogy and Petrology* **107**, 202–18.

Petford, N. 2003. Rheology of granitic magmas during ascent and emplacement. *Annual Review of Earth and Planetary Sciences* **31**, 399–427.

Petford, N. Clemens, J. D. & Vigneresse, J. L. 1997. Application of information theory to the formation of granitic rocks. *In* Bouchez, J. L., Hutton, D. & Stephens, W. E. (eds) *Granite: from Melt Segregation to Emplacement Fabrics*, 3–10. Dordrecht: Kluwer Academic Publishers.

Petford, N., Cruden, A. R., McCaffrey, K. J. W. & Vigneresse, J. L. 2000. Granite magma formation, transport and emplacement in the Earth's crust. *Nature* **408**, 669–73.

Petford, N. & Gallagher, K. 2001. Partial melting of mafic (amphibolitic) lower crust by periodic influx of basaltic magma. *Earth and Planetary Science Letters* **193**, 483–99.

Pitcher, W. 1979. The nature, ascent and emplacement of granitic magmas. *Journal of the Geological Society, London* **136**, 627–62.

Pitcher, W. S. 1987. Granites and yet more granites forty years on. *Geologische Rundschau* **76**, 51–79.

Pitcher, W. S. 1993. *The nature and origin of granite.* London: Chapman & Hall.

Pitcher, W. S., Atherton, M. P., Cobbing, E. J. & Beckinsale, R. D. 1985. *Magmatism at a Plate Edge: The Peruvian Andes.* Glasgow: Blackie.

Pitcher, W. S. & Hutton, D. H. W. 1982. Discussion on a tectonic model for the emplacement of the Main Donegal Granite, N.W. Ireland: *Journal of the Geological Society, London* **141**, 599–602.

Pollard, D. D. & Muller, O. H. 1976. The effect of gradients in regional stress and magma pressure on the form of sheet intrusions in cross section. *Journal of Geophysical Research* **B81**, 975–84.

Pons, J., Barbey, P., Dupuis, D. & Léger, J. M. 1995. Mechanisms of pluton emplacement and structural evolution of a 2·1 Ga juvenile continental crust: the Birimian of southwestern Niger. *Precambrian Research* **70**, 281–301.

Rabinowicz, M., Genthon, P., Ceuleneer, G. & Hillairet, M. 2001. Compaction in a mantle mush with high melt concentrations and the generation of magma chambers. *Earth and Planetary Science Letters* **188**, 313–28.

Rabinowicz, M. & Vigneresse, J. L. 2004. Melt segregation under compaction and shear channelling: Application to granitic magma segregation in a continental crust. *Journal of Geophysical Research* **B109**, 10.1029/2002JB002372.

Rapp, R. P. 1995. Amphibole-out phase boundary in partially melted metabasalt, its control over liquid fraction and composition, and source permeability. *Journal of Geophysical Research* **B100**, 15601–10.

Rapp, R. P. & Watson, E. B. 1995. Dehydration melting of metabasalt at 8–32 kbar: Implications for continental growth and crust-mantle recycling. *Journal of Petrology* **36**, 891–931.

Read, H. H. 1957. *The granite controversy.* London: Thomas Murby and Co.

Renner, J., Evans, B. & Hirth, G. 2000. On the rheologically critical melt fraction. *Earth and Planetary Science Letters* **181**, 585–94.

Roberts, M. P. & Clemens, J. D. 1995. Feasability of AFC models for the petrogenesis of calc-alkaline magma series. *Contributions to Mineralogy and Petrology* **121**, 139–47.

Roscoe, R. 1952. The viscosity of suspensions of rigid spheres. *British Journal of Applied Physics* **3**, 267–9.

Rosenberg, C. L. 2001. Deformation of partially-molten granite: A review and comparison of experimental and natural case studies. *International Journal of Earth Sciences* **90**, 60–76.

Rosenberg, C. L. & Handy, M. R. 2000. Syntectonic melt pathways during simple shearing of a partially molten rock analogue (Norcamphor Benzamide). *Journal of Geophysical Research* **B105**, 3135–49.

Rosenberg, C. L. & Handy, M. R. 2001. Mechanisms and orientation of melt segregation paths during pure shearing of a partially molten rock analog (norcamphor–benzamide). *Journal of Structural Geology* **23**, 1917–32.

Rosenberg, C. L. & Handy, M. R. 2005. Experimental deformation of partially melted granite revisited: implications for the continental crust. *Journal of Metamorphic Geology* **23**, 19–28.

Rutter, E. H. & Neumann, D. H. K. 1995. Experimental deformation of partially molten Westerly granite under fluid-absent conditions with implications for the extraction of granitic magmas. *Journal of Geophysical Research* **B100**, 15697–716.

Stephens, W. E. 1992. Spatial, compositional and rheological constraints on the origin of zoning in the Criffel pluton Scotland. *Transactions of the Royal Society of Edinburgh: Earth Sciences* **83**, 191–9.

Stevenson, D. J. 1989. Spontaneous small scale melt segregation in partial melts undergoing deformation. *Geophysical Research Letters* **16**, 1067–70.

Taylor, S. R. & McLennan, S. M. 1995. The geochemical evolution of the continental crust. *Reviews of Geophysics* **33**, 241–65.

Thom, R. 1980. *Modèles Mathématiques de la Morphogénèse.* Paris: Christian Bourgeois.

Thompson, A. B. 1999. Some time-space relationships for crustal melting and granitic intrusion at various depths. *In* Castro, A., Fernandez, C. & Vigneresse, J. L. (eds) *Understanding Granites: Integrating New and Classical Techniques. Geological Society, London, Special Publication* **168**, 7–25.

Vernon, R. H. 1990. Crystallization and hybridism in microgranitoid enclave magmas: microstructural evidence. *Journal of Geophysical Research* **B95**, 17849–59.

Vigneresse, J. L. 2004. Toward a new paradigm for granite generation. *Transactions of the Royal Society of Edinburgh: Earth Sciences* **95**, 11–22.

Vigneresse, J. L., Barbey, P. & Cuney, M. 1996. Rheological transitions during partial melting and crystallisation with application to felsic magma segregation and transfer. *Journal of Petrology* **37**, 1579–600.

Vigneresse, J. L., Tikoff, B. & Améglio, L. 1999. Modification of the regional stress field by magma intrusion and formation of tabular granitic plutons. *Tectonophysics* **302**, 203–24.

Vigneresse, J. L. & Burg, J. P. 2000. Continuous versus discontinuous melt segregation in migmatites: insights from a cellular automaton model. *Terra Nova* **12**, 188–92.

Vigneresse, J. L. & Burg, J. P. 2004. Some insights on the rheology of partially molten rocks. *In* Grocott, J., McCaffrey, K., Taylor, G. & Tikoff, B. (eds) *Vertical Coupling and Decoupling in the Lithosphere. Geological Society, London, Special Publication* **272**, 327–36.

Vigneresse, J. L. & Burg, J. P. 2005. Simulation of crustal melt segregation through cellular automata: Insight on steady and non-steady state effects under deformation. *Pageoph* **162**, 987–1011.

Vigneresse, J. L. & Tikoff, B. 1999. Strain partitioning during partial melting and crystallizing felsic magmas. *Tectonophysics* **312**, 117–32.

Wall, V. J., Clemens, J. D. & Clarke, D. B. 1987. Models for granitoid evolution and source compositions. *Journal of Geology* **95**, 731–49.

Walte, N. P., Bons, P. D. & Passchier, C. W. 2005. Deformation of melt-bearing systems – insight from in situ grain-scale analogue experiments. *Journal of Structural Geology* **27**, 1666–79.

Weaver, B. L. & Tarney, J. 1980. Continental crust composition and nature of the lower crust: constraints from mantle Nd-Sr isotope correlation. *Nature* **286**, 342–6.

Webb, S. L. & Dingwell, D. B. 1990. Non-Newtonian rheology of igneous melts at high stresses and strain rates: Experimental results for rhyolite, andesite, basalt and nephelinite. *Journal of Geophysical Research* **B95**, 15695–701.

Weinberg, R. F., Sial, A. N. & Pessoa, R. R. 2001. Magma flow within the Tavares pluton, northeast Brazil: Compositional and thermal convection. *Geological Society of America Bulletin* **113**, 508–20.

Whitney, J. A. 1990. Origin and evolution of silicic magmas. *Reviews in Economic Geology* **4**, 183–201.

Williams, P. F. 1990. Differentiated layering in metamorphic rocks. *Earth-Science Reviews* **29**, 267–81.

Yoshinobu, A. S. & Hirth, G. 2002. Microstructural and experimental constraints on the rheology of partially molten gabbro beneath oceanic spreading centers. *Journal of Structural Geology* **24**, 1101–7.

JEAN LOUIS VIGNERESSE, Nancy Université, UMR CNRS 7566 G2R, BP 23, Vandoeuvre-les-Nancy Cedex, F-54501 France.
e-mail: jean-louis.vigneresse@g2r.uhp-nancy.fr

MS received 2 February 2006. Accepted for publication 3 April 2007.